Therapeutic Effects of Targeted PPARɣ Activation on Inflamed High-Risk Plaques Assessed by Serial Optical Imaging In Vivo

Jah Yeon Choi[1,*], Jiheun Ryu[2,*], Hyun Jung Kim[1,*], Joon Woo Song[1], Joo Hee Jeon[1], Dae-Hee Lee[3], Dong Joo Oh[1], Dae-Gab Gweon[2], Wang-Yuhl Oh[2], Hongki Yoo[4,†], Kyeongsoon Park[5,†], Jin Won Kim[1,†]

Running Title: Targeted Activation of PPARɣ Pathway

[1]Multimodal Imaging and Theranostic Lab, Cardiovascular Center, Korea University Guro Hospital, Seoul, Republic of Korea, 152-703

[2]Department of Mechanical Engineering, KAIST, Daejeon, Republic of Korea, 305-701

[3]Division of Medical Oncology, Department of Internal Medicine, Korea University Guro Hospital, Seoul, Republic of Korea, 152-703

[4]Department of Biomedical Engineering, Hanyang University, Seoul, Republic of Korea, 133-791

[5]Department of Systems Biotechnology, College of Biotechnology and Natural Resources, Chung-Ang University, Anseong-si, Gyeonggi-do, Republic of Korea, 17546

*JYC, JR, HJK contributed equally to this work.

† Shared corresponding author, Email: kjwmm@korea.ac.kr,

METHODS

Synthesis of MMR-Lobe

MMR-targeting carriers as a lobeglitazone (Chong Kun Dang Pharmaceutical Corp.) delivery system were prepared as described in the previous study[1]. Briefly, thiolated glycol chitosan (tGC, 400 mg) and mannose-polyethylene glycol-maleimide (MAN-PEG-MAL; m/z = approximately 2,479.3 Da) were reacted in PBS (70 mL, pH 6.9) for 20 h, dialyzed against distilled water using a dialysis membrane (MWCO 12,000–14,000 Da, Spectrum) for 2 days, and lyophilized to yield MAN-PEG-GC. To fabricate self-assembled structures, MAN-PEG-GC (100 mg) and cholesteryl chloroformate (5 mg, Sigma) were reacted in anhydrous dimethyl sulfoxide (DMSO, Sigma):dimethylforamide (DMF, Sigma) co-solvent (3:1, v/v, 20 mL) containing triethylamine (9 μL, Sigma) for 24 h. For *in vivo* imaging and monitoring drug efficacy in atherosclerotic plaques, Cyanine 5.5 (Cy5.5)-NHS ester (2 mg, Lumiprobe) was further added and reacted in darkness overnight. The mixture was then dialyzed against deionized water:ethanol (1:2, v/v) for 2 days using a dialysis membrane (MWCO 12,000–14,000 Da) and further dialyzed against distilled water for additional 2 days, and freeze-dried to obtain MMR-targeting particles or MMR-targeting probes labeled with Cy5.5. For assessing anti-atherogenic effects, lobeglitazone-loaded MMR-targeting particles were prepared as follows: MMR-targeting particles (100 mg) and lobeglitazone (30 mg) were clearly dissolved in DMSO by stirring for 3 h, dialyzed against distilled water using a dialysis membrane (MWCO 6,000–8,000 Da) for 1 day, and lyophilized for 2 days to obtained lobeglitazone-loaded MMR-targeting particles (MMR-Lobe).

Characterizations of MMR-Lobe

To evaluate shapes and sizes of MMR-Lobe, 1 mg of MMR-Lobe was dispersed in distilled water (1 mL) by 1 min of vortexing and 1 min of sonification (100 W). Then, the dispersed MMR-Lobe particles were analyzed with a Zetasizer 3000 instrument (Malvern Instruments) and an Energy Filtering Transmission Electron Microscope (EF-TEM, LEO 912AB OMEGA, Carl Zeiss, Germany) to determine shape and size, respectively.

To determine the uptake of MMR probes in macrophage derived foam cells, RAW 264.7 cells were stimulated with low-density lipoprotein (LDL, 100 μg/mL) and lipopolysaccharide (LPS, 200 ng/mL). After 24 h, cells were replaced with fresh media containing various concentrations of MMR-Cy5.5 (25, 50, and 100 μg/mL) for 1 h. The cells were washed two times with PBS to remove MMR-Cy5.5 that were not internalized and fixed with paraformaldehyde solution for 30 min. After nuclei of the cells were stained with DAPI for 10 min and the cellular uptake was visualized using intravital multi-photon laser-scanning confocal microscope (LSM 780 Meta NLO, Carl Zeiss, Germany).

The drug loading efficiency and loading content of lobeglitazone in the MMR-Lobe were calculated by first dissolving the MMR-Lobe (1 mg) in 1 mL of acetonitrile:H_2O:formic acid (60:40:0.25, v/v/v). The amount of lobeglitazone in the MMR-Lobe was determined by HPLC (Agilent 1260 series). To analyze loading efficiency and loading content using HPLC, the mobile phase was acetonitrile:H_2O:formic acid (60:40:0.25), with a flow rate of 0.5 mL/min. The sample injection volume was 5 μL and detected at 250 nm. Loading efficiency and loading content were calculated by following equations:

$$Loading\ efficiency\ (\%) = \frac{\text{Weight of loaded drug}}{\text{Weight of initial feed drug}} \times 100$$

$$Loading\ content\ (\%) = \frac{\text{Weight of loaded drug}}{\text{Weight of molecules}} \times 100$$

In vitro drug release studies

To study the *in vitro* release profile of lobeglitazone from MMR-Lobe, the lyophilized MMR-Lobe (1 mg) was dispersed in PBS (1 mL, pH 7.4) by 1 min of vortexing and 1 min of sonification (100 W). The dispersed MMR-Lobe was then placed in a dialysis membrane (MWCO 6,000–8,000 Da) which was immersed in 20 mL of PBS (pH 7.4) followed by gentle shaking in a water bath (37°C) oscillating 100 times/min. The medium was replaced with fresh medium at predetermined times. The amount of lobeglitazone released from MMR-Lobe was determined by HPLC in the same manner used for determining drug loading efficiency.

Macrophage foam cell formation and lipid staining

RAW 264.7 cells, derived from murine macrophages, were obtained from ATCC (Manassas, VA, USA). RAW 264.7 cells were cultured in Dulbecco's modified Eagle medium (DMEM; GenDEPOT) supplemented with 10% heat-inactivated fetal bovine serum (GenDEPOT), 100 U/mL penicillin and 100 μg/mL streptomycin (GenDEPOT). The cells were incubated in an atmosphere of 5% CO_2 at 37°C and were subcultured every 2 days.

RAW 264.7 cells were treated with lobeglitazone at 10 or 50 μM; MMR-Lobe containing 14.42 μg/mL or 72.10 μg/mL of MMR vehicle and 10 or 50 μM of lobeglitazone; MMR vehicle at 14.42 μg/mL or 72.10 μg/mL; or saline control. Foam cells were induced by treating with low-density lipoprotein (LDL, 100 μg/mL, Merck Millipore) for 18 h before stimulation with LPS (200 ng/mL), which promotes foam cell formation [2], for 24 h. The treated cells were

fixed with 3.8% formaldehyde (DANA Korea) for 40 min, followed by staining with Oil Red O (ORO; ScyTek Laboratories, USA) overnight at room temperature.

Macrophage foam cell formation was observed using an optical microscope (Olympus), and images were captured digitally in real time using a light microscope. Semi-quantitative analysis was performed by histogram analysis with Image J software. The stained area was measured and averaged for 30 cells in 10 fields per dish.

Measurement of pro-inflammatory cytokine (TNF-α, IL-6, MMP-9) production

RAW 264.7 cells were seeded into 60 mm dishes (5×10^5 cells/dish). Cells were pretreated with lobeglitazone at 10 or 50 μM; MMR-Lobe containing 14.42 μg/mL or 72.10 μg/mL of MMR vehicle and 10 or 50 μM of lobeglitazone; MMR vehicle at 14.42 μg/mL or 72.10 μg/mL; or saline control for 6 h, and were stimulated with LPS (100 ng/mL). After 3 h, the cell-free supernatants were collected and the levels of inflammatory cytokines (TNF-α, IL-6, MMP-9) were measured by a commercial enzyme-linked immunosorbent assay kit (ELISA; R&D systems, Minneapolis, Minnesota, USA).

Western blot analysis

RAW 264.7 cells were plated at a density of 5×10^6 cells per 100 mm dish. Cells were pretreated with lobeglitazone at 10 or 50 μM; MMR-Lobe containing 14.42 μg/mL or 72.10 μg/mL of MMR vehicle and 10 or 50 μM of lobeglitazone; MMR vehicle at 14.42 μg/mL or 72.10 μg/mL; or saline control. After 9 h of incubation, the cells were collected and washed twice with cold PBS. The cells were lysed in RIPA lysis buffer (Thermo Scientific, Rockford,

IL, USA) and kept on ice for 30 min. Cell lysates were washed by centrifugation, and protein concentrations were determined using a BCA protein assay kit (Thermo Scientific, Rockford). Lysate aliquots (40 μg total protein) were separated on 10% SDS-polyacrylamide gels and transferred onto polyvinylidene fluoride (PVDF) membranes (EMD Millipore, Billerica, MA, USA) with a glycine transfer buffer (Bio-Rad, CA). After blocking nonspecific sites with 5% blotting-gradient blocker (Bio-Rad, CA) in 1X TBS-T, the membrane was then incubated with the appropriate specific primary antibody (ABCA1, ABCG1, or LXRα from NOVUS Biological) at 4°C overnight. The membrane was further incubated for 1 h with the appropriate peroxidase-conjugated secondary antibody (1:3000; Santa Cruz Biotechnology Inc.) at room temperature. The immune-active proteins were detected using an enhanced chemiluminescence western blotting detection kit (Thermo Scientific).

Real-time PCR

RAW 264.7 cells were plated at a density of 5×10^6 cells per 6-well plate. Cells were pretreated with lobeglitazone at 10 or 50 μM; MMR-Lobe containing 14.42 μg/mL or 72.10 μg/mL of MMR vehicle and 10 or 50 μM of lobeglitazone; MMR vehicle at 14.42 μg/mL or 72.10 μg/mL; or saline control. After incubation, total RNA was isolated from RAW 264.7 cells using an eCube Tissue RNA mini kit according to the manufacturer's instructions (PhileKorea Technology). The mRNA levels of ABCA1, ABCG1, and LXRα were assessed by Real time PCR.

Total RNA was converted into cDNA using QuantiSpeed SYBR One-step Hi-ROX kit (PhileKorea Technology) by following the manufacturer's instruction. cDNAs were amplified and detected using SYBR Green chemistry (PhileKorea Technology) in an ABI 7300 Real time

PCR system (Applied Biosystems).

The targeted genes and primer sequences are as follows: ABCA1: forward primer: 5'-GCGGACCTCCTGGGTGTT-3', Reverse primer: 5'-CAAGAATCTCCGGGCTTTA-GG-3'; ABCG1: forward primer: '-AAGGCCTACTACCTGGCAAAGA-3', Reverse primer: 5'-GCAGTAGGCCACAGG-GAACA-3'; LXRα: forward primer: 5'-CCTTCCTCAAGGACTT

CAGTTACAA-3', Reverse primer: 5'-CATGGC-TCTGGAGAACTCAAAGAT-3'; GAPDH: forward primer: 5'-CCACCCATGGCAAATTCC-3', Reverse primer: 5'-TGGGAT-TTCCATTGATGACAAG-3'. Measurements were quantitated using the Ct method and GAPDH expression was used as the internal control. All samples were run in triplicate.

Quantification of cholesterol levels in macrophage derived foam cells.

The levels of total cholesterol in macrophage foam cells were measured using a commercially available assay kit (Cell Biolabs Inc, San Diego, CA, USA). This is a fluorometric assay, which involves the extraction of total cholesterol with chloroform: isopropanol: NP-40(7: 11:0.1).

Animal model and study protocol

All animal experiments were approved by the Korea University Institutional Animal Care & Use Committee (KUIACUC-2015-197) in accordance with institutional guidelines. Eight-week-old male apoE$^{-/-}$ mice (B6.129P2-Apoetm1Unc/J, Jackson laboratory) were fed a high cholesterol diet (D12336, Research Diets Inc., USA) for 8 weeks to induce atherosclerosis. All mice were imaged on a custom-built intravital fluorescence microscope for baseline carotid image, and subsequently were treated for 4 week with intravenous injection of MMR-Lobe (7

mg/kg; 2 injections per week, N= 7), or oral administration of lobeglitazone (2 mg/kg per day, N= 6), MMR vehicle (2 MMR vehicle injections per week, n = 6), or placebo (2 saline injections per week, N= 6). Mice were maintained on a normal diet during the treatment. After 4 weeks of treatment, the same carotid atheromata visualized previously underwent a second *in vivo* imaging using the same protocol. After 2nd imaging, *ex vivo* en face aorta imaging and comprehensive immuohistological analysis were performed.

For *in vivo* imaging, MMR-Cy5.5 (10 mg/kg) in saline (150 μL) was injected into mice via tail vein 48 h prior to imaging. The mice were anesthetized by intraperitoneal injection of a mixture of Zoletil (30 mg/kg) and Rompun (10 mg/kg). Before imaging, FTIC-dextran was administered via tail vein as an angiographic fluorescent imaging agent. The carotid artery was surgically exposed and a mechanical stabilizer was placed underneath the carotid artery bifurcation for reducing artifacts from respiratory and cardiac motion as well as for a co-registration marker between the first and second *in vivo* imaging sessions. Bright-field images of carotid artery were acquired using a Sony NEX-5 digital camera for subsequent determination of the imaging site.

Multi-Channel confocal intravital optical imaging

A custom-built multi-channel confocal intravital fluorescence microscope (MCC-IVFM) was used to visualize macrophage distribution *in vivo*. The MCC-IVFM instrument was optimized for *in vivo* imaging of murine carotid arteries with its upright epi-fluorescence configuration for convenient access to the carotid artery, fast image acquisition rate of 4 frames/s (1024 × 1024 pixels) using a 4-kHz resonant scanner (CRS-4kHz, Cambridge Technology, Bedford, MA), wide field-of-view of 2.4 mm × 2.4 mm by using a 10×/0.3-NA objective lens

(UPlanFLN, Olympus, Japan), highly sensitive signal detection using a GaAsP photomultiplier tube (H7422P-40, Hamamatsu Photonics, Japan), and flexible access to the target area using a 5-axis staging platform.

To demonstrate the efficacy of our PPARγ agonist (lobeglitazone)-loaded MMR probe, all settings of the IVFM such as the magnification, field-of-view, detector gain, confocal pinhole size (MPH16, Thorlabs), and the number of images averaged, were recorded for every mouse. Bright-field images were acquired to co-register the imaging fields of 2 IVFM data sets. To simultaneously visualize the plaque macrophage distribution and carotid angiogram, 633 nm and 488 nm excitation lasers were used for macrophage mannose receptor targeting cyanine probe (MMR-Cy5.5) and FITC-dextran, respectively. The set of multiband dichroic beam-splitter (Di-R488/543/635, Semrock), multiband emission filter (FF01-515/588/700, Semrock) and fiber-coupled beam combiner (SFO555-001 3× RGB combiner, SIFAM) were used to provide the collinear beam-path for multiple wavelength channels. To enhance imaging quality, pulsation-induced motion artifacts were smoothed by averaging three to ten sequential images. The upper portion of the exposed carotid artery was imaged entirely by stacking multiple axially scanned images. The axial 400-μm range was scanned by 5-μm steps using a piezoelectric objective positioner (MIPOS 500, Piezosystem Jena GmbH). Also, three-dimensional images were reconstructed using ImageJ software (US National Institute of Health, Bethesda, MD).

Identification of macrophage-induced fluorescence signals

To quantify the macrophage-induced fluorescence signal generated by the MMR-NIRF probe, we applied threshold levels to each grayscale fluorescent image to remove background

auto-fluorescence. The average auto-fluorescence signal level was measured from four CL57BL/6 mice with various detector gain values. An equation to calculate the relationship between auto-fluorescence level and detector gain was obtained by 2nd order polynomial fitting using the least-squared-method (LSM) and the obtained r-squared value was over 0.999. The quantified threshold level was used for identifying whether each pixel value contains MMR-induced signal or not. Then, auto-fluorescence was eliminated from images without distorting the MMR fluorescence signals (Figure S4).

To investigate changes of MMR distribution in plaque regions between baseline and serial images of each apoE$^{-/-}$ mouse, the plaque boundaries were identified using the signal distribution of the FITC-dextran angiogram. Then, the effective macrophage area and the average macrophage signal intensity were calculated using the raw intensity data of the defined plaque region. In detail, the number of effective pixels where the signal intensity was higher than the applied threshold level, was converted into the effective mac area, A (mm^2) using the equation, $A = N \times (F / P)^2$, where N = the number of effective pixels which has macrophage signal higher than the threshold in the plaque region, F = the field-of-view size of the image in mm, and P = the number of pixels composing the field-of-view. Then, the average intensity of the mac signal, which was defined as the mean value of the plaque region, was calculated by averaging the intensity values of effective pixels used for the area calculation.

***Ex vivo en face* fluorescence reflectance imaging (FRI)**

Mice were euthanized by CO_2 inhalation at the end of the *in vivo* imaging procedure. Arterial tissues of euthanized mice were flushed with saline, and then harvested from the ascending to descending aorta. Peri-adventitial connective tissues were clearly separated from the vessel and

the aorta was opened longitudinally by an incision along the ventral aspect. The aorta was pinned out flat, luminal surface up, on a black silicone pad.

Near-infrared signal of the arterial plaque was measured using FRI followed by staining for lipids with Oil Red O (ORO; ScyTek Laboratories, USA) to measure the ORO-positive plaque area. *Ex vivo* fluorescence reflectance imaging (FRI) was performed using the Davinch *in vivo* Imaging System (Davinch-K Co., Ltd, Korea). To measure Cy5.5 signal intensity in the plaques, excitation and emission filters were set to 655 ± 20 nm and 716 ± 20 nm, respectively. The exposure time was 10 sec. Quantification of the signal intensity and aortic lumen area was performed with ImageJ software. Mean signal intensity divided by total area of the *en face* pinned-open aortas was used to compare results between groups.

After the *en face* FRI imaging, the whole aorta tissue was fixed with formalin at room temperature for 3 h, then washed overnight in PBS at 4°C. Aortas were dehydrated in room temperature propylene glycol for 5 min and then incubated in Oil Red O solution for 3 h at room temperature. Tissues were incubated in in 85% propylene Glycol three to four times, and washed overnight in PBS at 4°C. At the end of the staining procedure, lipid-containing plaques appeared red. To compare the ORO-positive plaque areas among the three groups, red-stained plaque area divided by total aortic area was determined using ImageJ software.

Immunofluorescence staining

Fresh frozen aortic roots were embedded in optimum cutting temperature (O.C.T.) compound and stored at -70°C. Entire length of the aortic sinus region was serially cross-sectioned (10 μm thick). Frozen aortic valves fixed in 4% formaldehyde for 15 min at room temperature. After washed with PBST, aortic valves were blocked with peroxidase for 10 min at room

temperature. The following primary antibodies for PPARγ (1:50, rabbit anti-PPARγ, Novus Biological, USA), LXRα (1:50, rabbit anti-LXRα, Abcam, UK), ABCA1 (1:500, rabbit anti-ABCA1, Abcam, UK), ABCG1 (1:50, rabbit anti-ABCG1, Abcam, UK), and MMP-9 (1:500, rabbit anti-MMP9, Abcam, UK) were used. After incubating overnight at 4°C and washing with PBS for 15 min, aortic sinus sections were incubated with appropriate secondary antibodies for 2 h at 37°C: Alexa Fluor 488-conjugated goat anti-rabbit IgG (1:100, Jackson ImmuneResearch Laboratories, USA), Alexa Fluor 594-conjugated goat anti-rabbit IgG (1:100, Jackson ImmuneResearch Laboratories, USA), AMCA-conjugated goat anti-rabbit IgG (1:100, Jackson ImmuneResearch Laboratories, USA). The section were observed under a confocal laser scanning microscope (LSM700, Carl Zeiss, Germany) with identical windowing.

Histopathological validation

In vivo imaged carotid artery and aortic roots of each mouse were harvested and then flushed with normal saline to remove the blood from the vessel. Harvested tissues were embedded in O.C.T. compound and stored at -70°C. Entire length of the carotid artery and aortic sinus region was serially cross-sectioned (10 μm thick). For immunohistochemistry, the following primary antibodies were used: Mac3 (1:4,000, BD Pharmingen, USA); CD86 (1:50 dilution, cat.no 550542, BD Pharmingen, USA). ORO (30 min incubation, cat.no ORK-2, Scy Tek LABORATORIES, USA). Mac-3, and CD86 stained cross sections were detected with the Polink-2 HRP Plus Rat-NM DAB Detection System (GBI Labs, USA).

In carotid arteries, the three consecutive cross-sections of the largest plaque areas were adopted for analysis. Total 72 sections; 3 sections of largest plaque area per mouse, 6 mice per group were analyzed. Plaque macrophage or lipid stained areas were determined by the ratio

of Mac3- or ORO-positive areas to the intima areas of plaques. In atherosclerotic lesions of aortic sinus region, we evaluated 40 cross-sections of the aortic sinus area per mouse, which resulted in the analysis of 960 cross-sections in total, covering the entire aortic root. The largest plaque area of the three valve leaflets were used for morphological analysis. Every three consecutive cross-sections were subjected immunohistochemistry.

Statistical analysis

Statistical analyses were performed with GraphPad Prism (v5.3; GraphPad Software, San Diego, CA). Data are expressed as mean ± SD. Mean values were compared between four groups by a Kruskal–Wallis non-parametric one-way analysis of variance (ANOVA), and two-groups by a Mann-Whitney test. The Wilcoxon matched-pairs signed-ranks test was used to determine differences between the first and second images from the same murine carotid plaque. P values less than 0.05 were considered statistically significant.

REFERENCES

1. Kim JB, Park K, Ryu J, Lee JJ, Lee MW, Cho HS, et al. Intravascular optical imaging of high-risk plaques in vivo by targeting macrophage mannose receptors. Sci Rep. 2016; 6: 22608.
2. Hwang HJ, Chung HS, Jung TW, Ryu JY, Hong HC, Seo JA, et al. The dipeptidyl peptidase-IV inhibitor inhibits the expression of vascular adhesion molecules and inflammatory cytokines in HUVECs via Akt- and AMPK-dependent mechanisms. Mol Cell Endocrinol. 2015; 405: 25-34.

Figure Legends

Figure S1. Effects of MMR-probe on serum inflammatory cytokine production in CL57BL/6 mice. n = 7 mice per group; NS, not significant, by Mann-Whitney test.

Figure S2. The uptake of MMR-vehicle is mediated by mannose receptor binding. Mannose receptor blocking by D-mannose or mannan decreased MMR-Cy5.5 uptake in macrophage foam cells**.**

Figure S3. Inhibitory effect of MMR-Lobe on foam cell formation is mediated by mannose receptor binding. When mannose receptors are blocked with D-mannose or mannan, inhibitory effect of MMR-Lobe decreased and foam cell formation increased. Results were obtained from 3 separate experiments; * $P < 0.05$, ** $P < 0.01$, by ANOVA followed by Mann-Whitney test.

Figure S4. Identification of macrophage-induced fluorescence signals. To quantify the macrophage-induced fluorescent signal generated, we applied the thresholding that were obtained by averaging the levels of auto-fluorescence from four CL57BL/6 mice. The auto-fluorescence was eliminated from the images without distortion of the MMR fluorescence signals.

Figure S5. Representative images of aortic plaques co-stained with antibodies against PPARγ (green), LXRα (blue), ABCA1 (red), and ABCG1 (red) in control, MMR vehicle, and lobeglitazone treated group.

Figure S6. Double immunofluorescence stainings for macrophage/PPARγ, macrophage/ LXRα, macrophage/ABCA1, macrophage/ABCG1, and macrophage/MMP9 in aortic valve of MMR-lobe group.

Figure S1.

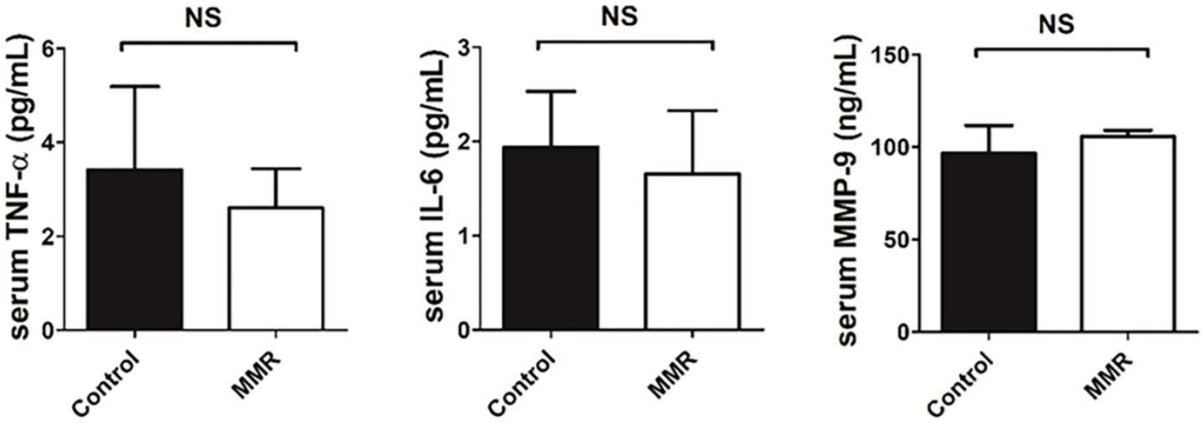

Figure S2.

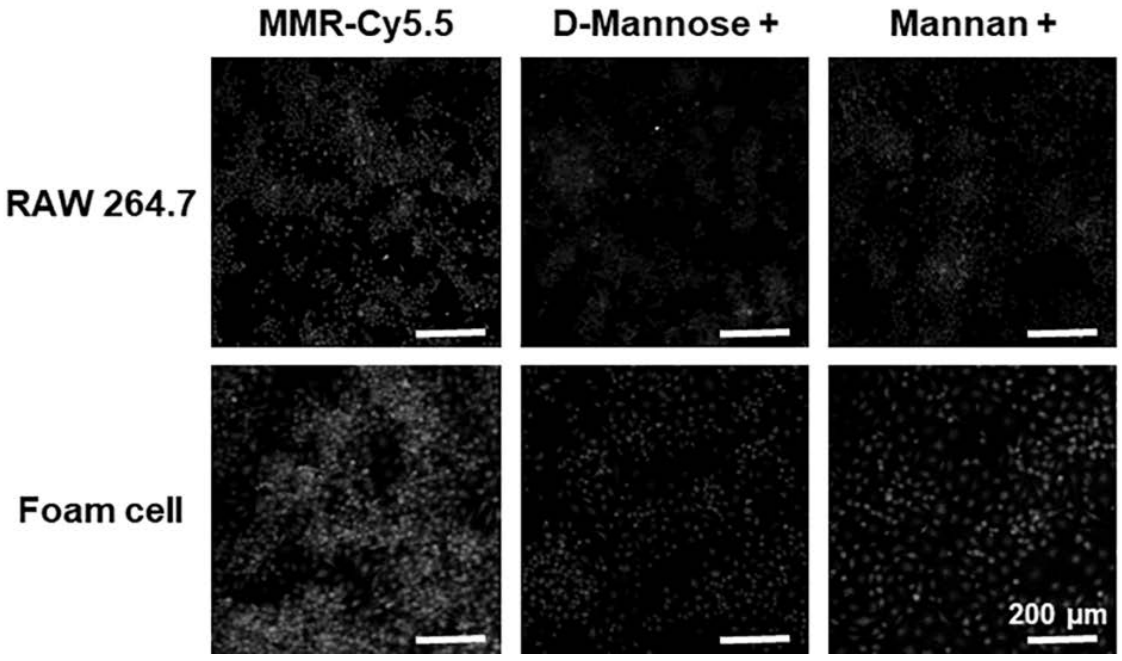

Figure S3.

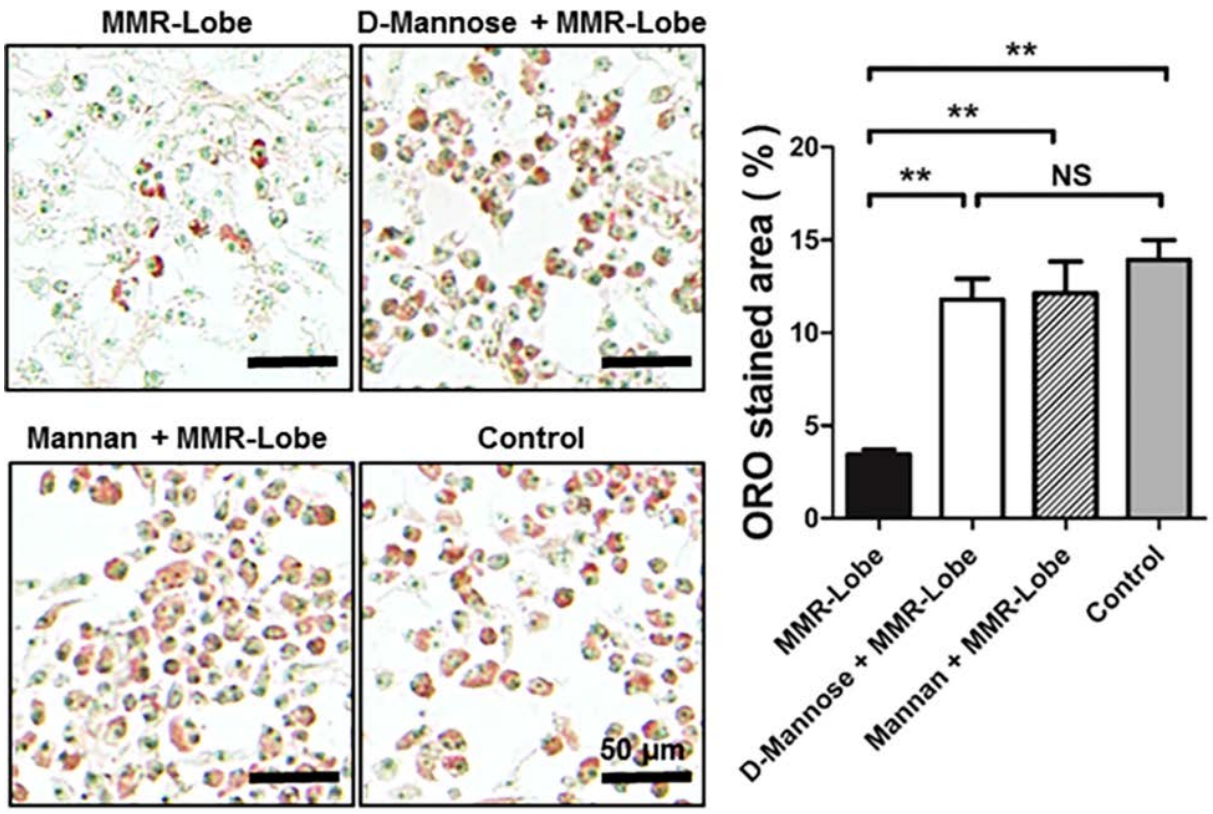
MMR-Lobe
D-Mannose + MMR-Lobe
Mannan + MMR-Lobe
Control
50 μm
ORO stained area (%)
0
5
10
15
20
**
**
**
NS
MMR-Lobe
D-Mannose + MMR-Lobe
Mannan + MMR-Lobe
Control

Figure S4.

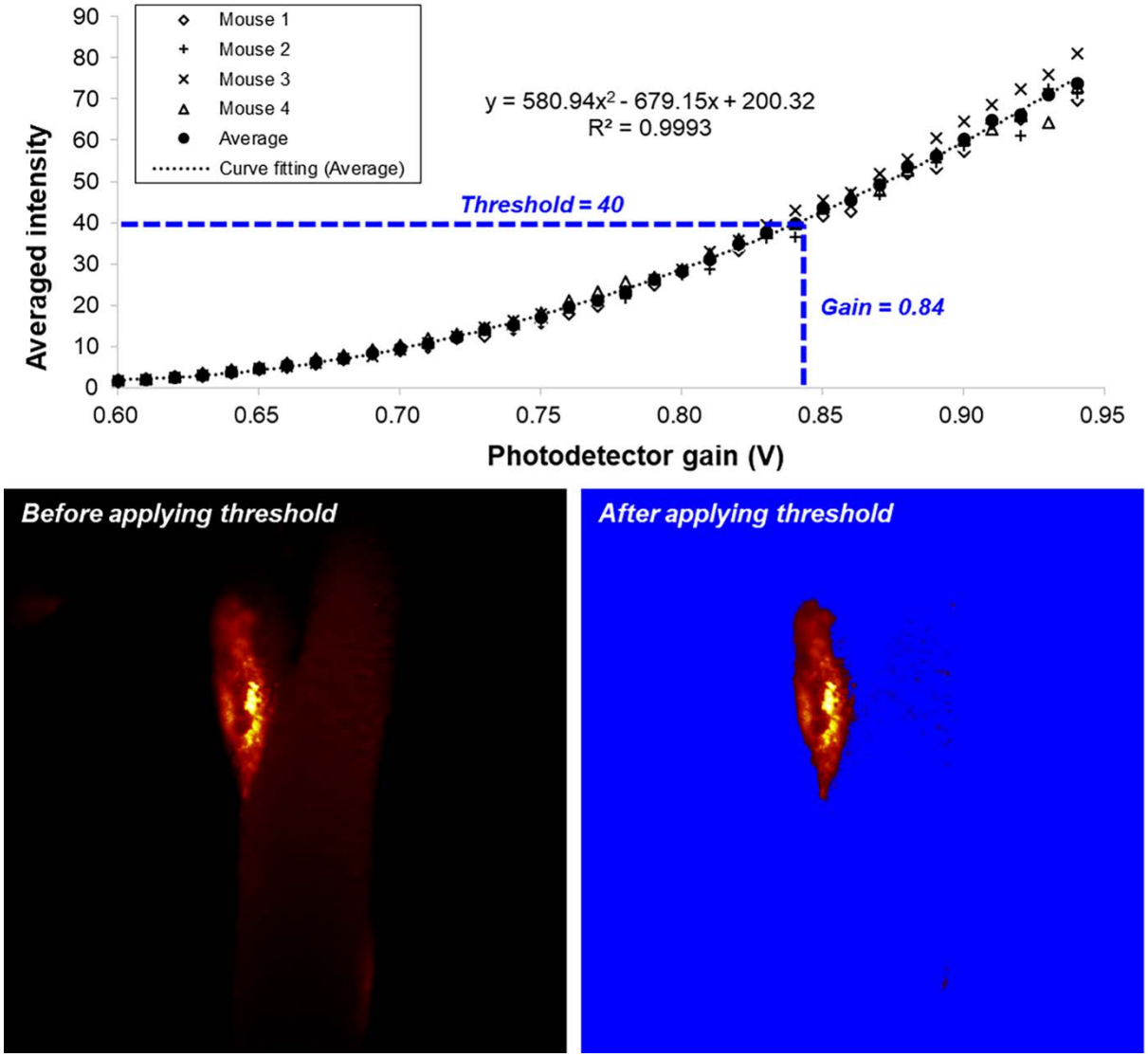
Mouse 1
Mouse 2
Mouse 3
Mouse 4
Average
Curve fitting (Average)
y = 580.94x² - 679.15x + 200.32
R² = 0.9993
Threshold = 40
Gain = 0.84
Averaged intensity
Photodetector gain (V)
0
10
20
30
40
50
60
70
80
90
0.60
0.65
0.70
0.75
0.80
0.85
0.90
0.95
Before applying threshold
After applying threshold

Figure S5.

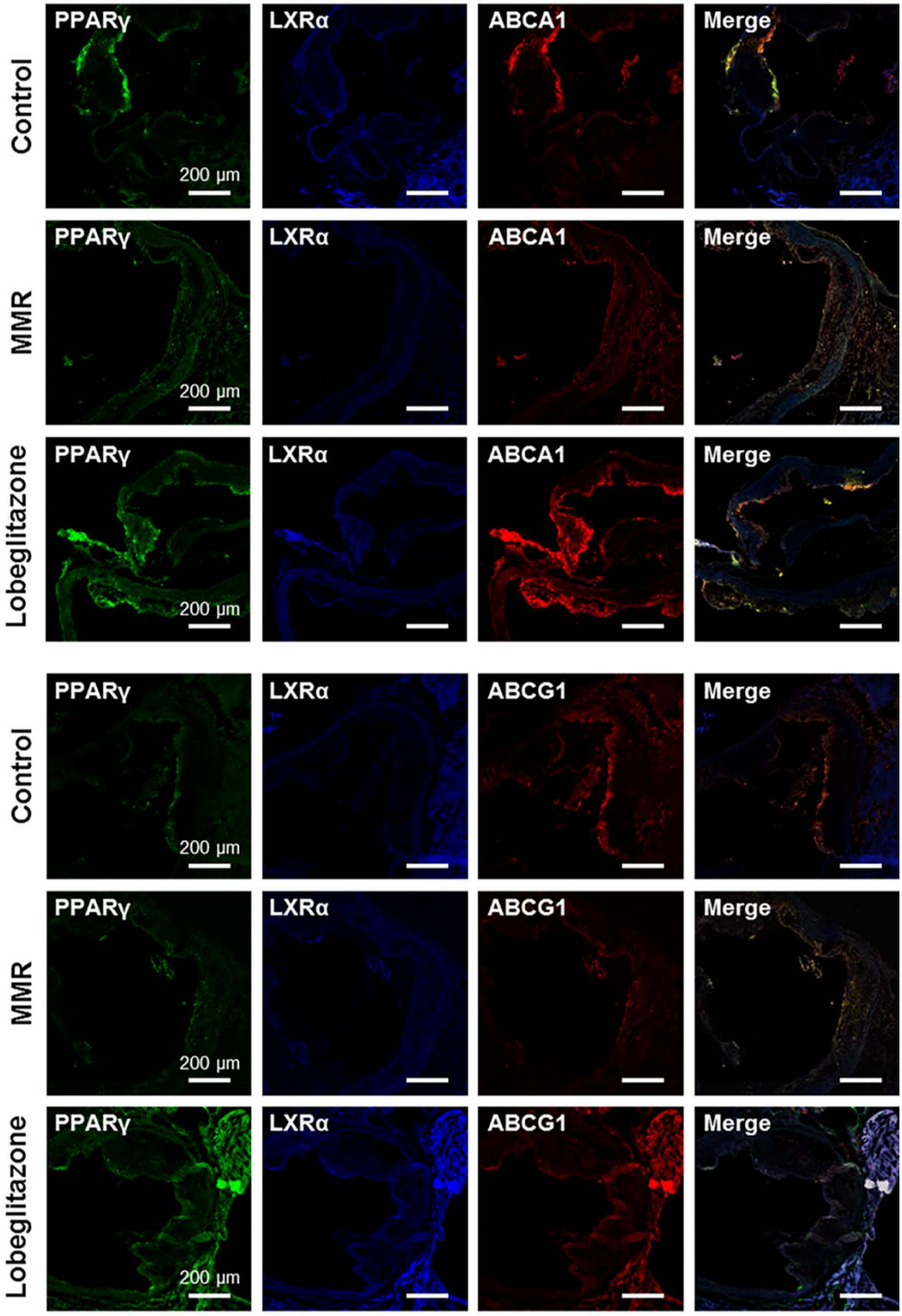
Control
MMR
Lobeglitazone
Control
MMR
Lobeglitazone
PPARγ
LXRα
ABCA1
ABCG1
Merge
200 μm

Figure S6.

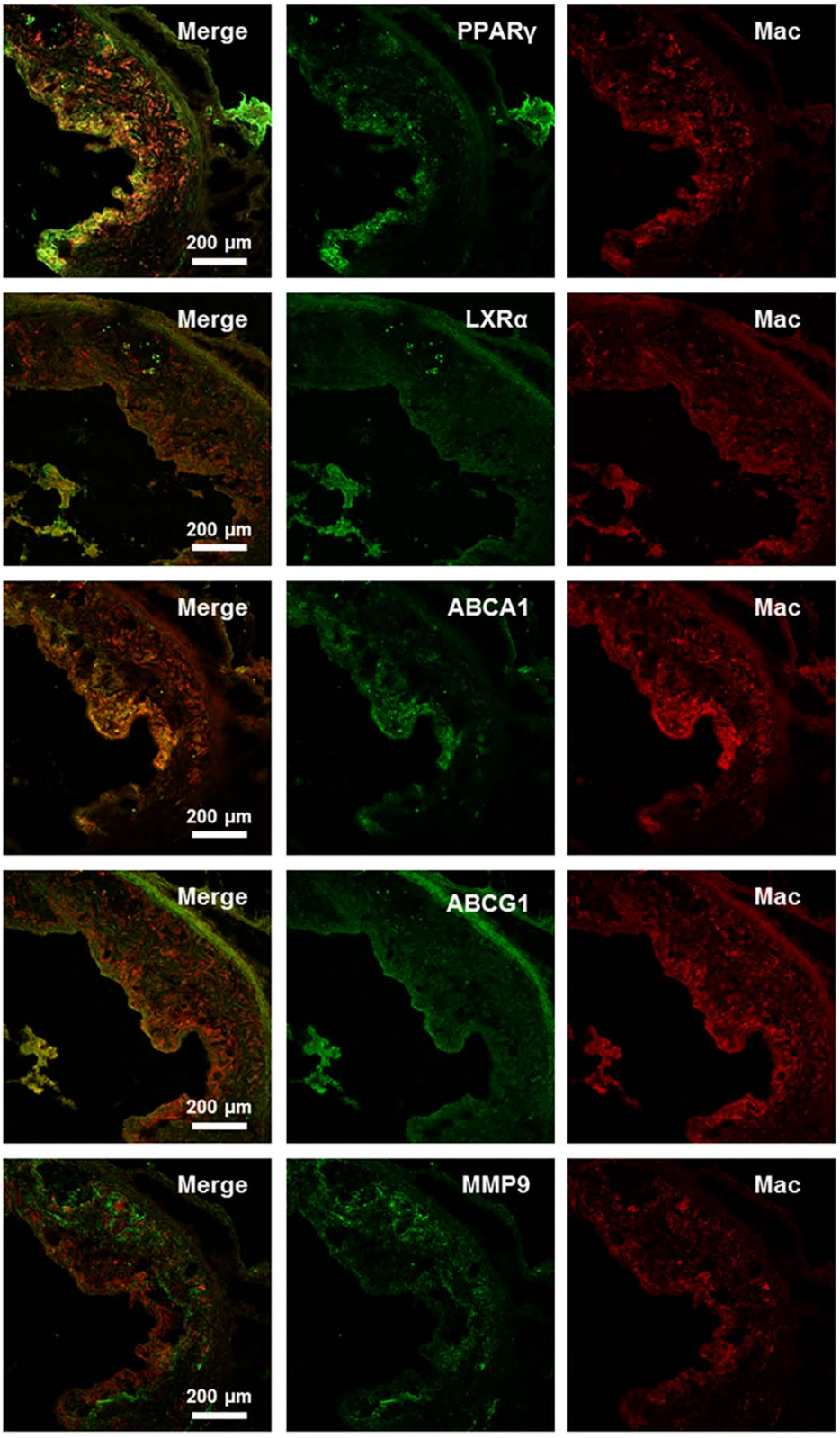
Merge
PPARγ
Mac
200 μm
Merge
LXRα
Mac
200 μm
Merge
ABCA1
Mac
200 μm
Merge
ABCG1
Mac
200 μm
Merge
MMP9
Mac
200 μm